Topological Control of Electron Localization in π-Conjugated Polyarylmethyl Carbopolyanions and Radical Anions

Suchada Utamapanya and Andrzej Rajca*,†

Contribution from the Department of Chemistry, Kansas State University, Manhattan, Kansas 66506. *Received May 17, 1991. Revised Manuscript Received July 26, 1991*

Abstract: The polyarylmethyl carbodecaanion $4^{10-}.10Li^+$ and its lower homologues can be considered as ensembles of uniformly charged, weakly interacting, arylmethyl anion fragments. Preparation of the carbopolyanions and their analysis by NMR spectroscopy, UV–vis spectroscopy, and electrochemistry are reported. The carbopolyanions are obtained by cleavage of the ether precursors with lithium in tetrahydrofuran. The mechanism of this reaction (for monoanions and dianions) is investigated using NMR, UV–vis, and ESR spectroscopy. Electron localization in the 1,3-connected polyarylmethyl $2^{\bullet-}.Li^+$ radical anion and delocalization in the 1,4-connected polyarylmethyl radical anion $7^{\bullet-}.Li^+$ on the ESR time scale is found.

Introduction

Mixed valence compounds have been essential to the understanding of fundamental aspects of electronic structure.[1-5] Almost all mixed valence compounds known to date are inorganic and, typically, possess two transition metal ions in different oxidation states connected together via a bridging ligand, e.g., pyrazine bridging Ru(III) and Ru(II) in the Creutz–Taube ion.[2-4] (μ-pyrazine)bis(pentaammineruthenium)(5+). Only very few organic mixed valence compounds are known.[6,7]

The problem of mixed valency can be generalized by considering the interaction between two (or more) weakly coupled moieties linked via a bridging unit as a function of the number of electrons, as shown in Scheme I. The results of the interaction between the moieties in each case are as follows: high- or low-spin ground state (case 1), localization or delocalization of charge and spin (case 2), and uniform or nonuniform charge distribution (case 3). The advantage of organic systems is that such interactions can be made strong and be studied without infraction from the complex electronic structure associated with transition metals: e.g., attempts to observe magnetic Ru(III)–Ru(III) interactions (intramolecular high- vs low-spin coupling between the metals) in derivatives of the Creutz–Taube ion were unsuccessful.[8]

Understanding electronic structure, which is associated with the high-spin coupling between electrons, is an important factor in the quest for organic magnets.[9] Several high-spin organic molecules have been prepared.[10-14b] *m*-Phenylene has been identified as one of the high-spin bridging units:[15] diradicals which contain the isomeric *p*-phenylene as a bridging unit have been found to possess a low-spin ground state.[16] It would be interesting to explore the effect of different topologies of the bridging unit for radical anions (case 2, Scheme I) and polyanions (case 3, Scheme I).

In two preliminary reports, we have described a tetraradical, $3^{4\bullet}$, and the corresponding tetraanion, $3^{4-}.4Li^+$ (Figure 1).[14] A question has been raised concerning whether the high spin (quintet) in the tetraradical is related to uniform charge distribution over triarylmethyl fragments in the tetraanion and its lower homologues.[14]

This paper elaborates on the relationship between high spin in polyradicals, uniform charge distribution in polyanions, and unusual electron localization in radical anions. We report the preparation of 1,3-connected polyarylmethyl decaanion $4^{10-}.10Li^+$ and tetraanion $5^{4-}.4Li^+$ to test for a uniform charge distribution over the arylmethyl fragments by extending conjugation and removing *t*-Bu substituents, respectively (Figure 2). Charge distribution in polyanions is studied using NMR and UV–vis spectroscopy and voltammetry. The mechanism of the reductive cleavage of polyethers using lithium in tetrahydrofuran (THF) is investigated, and radical anions are identified as intermediates. The ESR studies indicate electron localization in the 1,3-connected

Scheme I

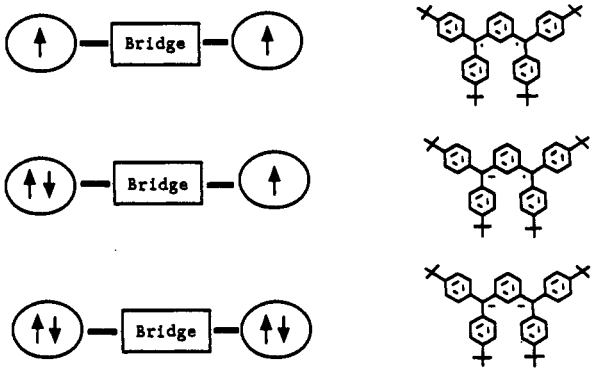

polyarylmethyl radical anion $2^{\bullet-}.Li^+$; for the corresponding 1,4-connected radical anions $7^{\bullet-}.Li^+$, electron delocalization is observed

† The Camille and Henry Dreyfus Teacher–Scholar, 1991.

(1) For reviews on inorganic mixed valence species, see: Hush, N. S. *Coord. Chem. Rev.* **1985**, *64*, 135. Creutz, C. *Prog. Inorg. Chem.* **1983**, *30*, 1. Brown, D. B. *Mixed-Valence Compounds*; Reidel: Dordrecht, The Netherlands, 1980.

(2) Creutz, C.; Taube, H. *J. Am. Chem. Soc.* **1969**, *91*, 3988. Creutz, C.; Taube, H. *J. Am. Chem. Soc.* **1973**, *95*, 1086.

(3) Piepho, S. B. *J. Am. Chem. Soc.* **1990**, *112*, 4197. Furholz, U.; Burgi, H. B.; Wagner, F. E.; Stebler, A.; Ammeter, J. H.; Krausz, E.; Clark, R. J. H.; Stead, M. J.; Ludi, A. *J. Am. Chem. Soc.* **1984**, *106*, 121. Stebler, A.; Ammeter, J. H.; Furholz, U.; Ludi, A. *Inorg. Chem.* **1984**, *23*, 2764. Furholz, U.; Joss, S.; Burgi, H. B.; Ludi, A.; *Inorg. Chem.* **1985**, *24*, 943.

(4) Oh, D. H.; Boxer, S. G. *J. Am. Chem. Soc.* **1990**, *112*, 8161. Joss, S.; Burgi, H. B.; Ludi, A. *Inorg. Chem.* **1985**, *24*, 949.

(5) Hage, R.; Haasnoot, J. G.; Nieuwenhuis, H. A.; Reedijk, J.; De Ridder, D. J. A.; Vos, J. G. *J. Am. Chem. Soc.* **1990**, *112*, 9245.

(6) Almlof, J. E.; Feyereisen, M. W.; Jozefiak, T. H.; Miller, L. L. *J. Am. Chem. Soc.* **1990**, *112*, 1206. Jozefiak, T. H.; Almlof, J. E.; Feyereisen, M. W., Miller, L. L. *J. Am. Chem. Soc.* **1989**, *111*, 4105.

(7) Nelsen, S. F.; Thompson-Colon, J. A.; Kaftory, M. *J. Am. Chem. Soc.* **1989**, *111*, 2809. Mazur, S.; Schroeder, A. H. *J. Am. Chem. Soc.* **1978**, *100*, 7339. Mazur, S.; Sreekumar, C.; Schroeder, A. H. *J. Am. Chem. Soc.* **1976**, *98*, 6713.

(8) Ru(III)–Ru(III) interactions: Johnson, E. C.; Callahan, R. W.; Eckberg, R. P.; Hatfield, W. E.; Meyer, T. J. *Inorg. Chem.* **1979**, *18*, 618. Bunker, B. C.; Drago, R. S.; Hendrikson, D. N.; Richman, R. M.; Kessell, S. L. *J. Am. Chem. Soc.* **1978**, *100*, 3805.

(9) *Proceedings of the Symposium on Ferromagnetic and High Spin Molecular Based Materials*; 197th National Meeting of the American Chemical Society, Dallas, TX, April, 1989. Miller, J. S.; Dougherty, D. A. *Mol. Cryst. Liq. Cryst.* **1989**, *176*, 1–562. Dougherty, D. A. *Acc. Chem. Res.* **1991**, *24*, 88.

(10) Poly(carbenes): Fujita, I.; Teki, Y.; Takui, T.; Kinoshita, T.; Itoh, K.; Miko, F.; Sawaki, Y.; Iwamura, H.; Izuoka, A.; Sugawara, T. *J. Am. Chem. Soc.* **1990**, *112*, 4074.

(11) Novak, J. A.; Jain, R.; Dougherty, D. A. *J. Am. Chem. Soc.* **1989**, *111*, 7618.

(12) Seeger, D. E.; Lahti, P. M.; Rossi, A. R.; Berson, J. A. *J. Am. Chem. Soc.* **1986**, *108*, 1251. Seeger, D. E.; Berson, J. A. *J. Am. Chem. Soc.* **1983**, *105*, 5144, 5146.

(13) Kirste, B.; Grimm, M.; Kurreck, H. *J. Am. Chem. Soc.* **1989**, *111*, 108.

0002-7863/91/1513-9242$02.50/0

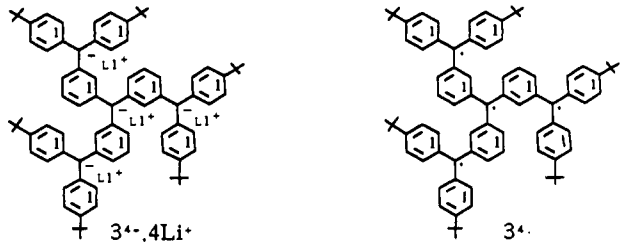

Figure 1. Structures of carbotetraanion 3^{4-},$4Li^+$ and tetraradical $3^{4\bullet}$.

under similar experimental conditions.

Results and Discussion

I. Carbopolyanions: NMR, UV–Vis, and Voltammetry. Carbopolyanions are obtained by vigorous stirring of the ether precursors in the presence of lithium metal in tetrahydrofuran (THF).[14a] Solutions of carbanions in THF (or THF-d_8), which contain equivalent amounts of EtOLi, are examined by NMR and UV–vis spectroscopy and voltammetry.

Quenching studies of the carbanions using MeOH and MeOD have been reported: the hydrocarbon products have been isolated in high chemical yields; NMR and FABMS analyses indicated >90% D incorporation for the deuterated products.[17]

NMR. The ^1H, ^{13}C, ^{13}C DEPT, and ^7Li NMR spectra for 1^-,Li^+, 2^{2-},$2Li^+$, 3^{4-},$4Li^+$ and ^1H–^1H COSY and ^6Li NMR spectra for 3^{4-},$4Li^+$ at 303 K have been reported in our preliminary communication.[14a] Those NMR studies are augmented by the generation and study of a carbodecaanion 4^{10-},$10Li^+$ and carbotetraanion 5^{4-},$4Li^+$. Also, variable-temperature and 2D NMR spectra are obtained.

Solutions of all carbopolyanions are examined by ^1H, $^{13}C\{^1H\}$, ^{13}C DEPT, ^6Li, ^7Li, and 2D NMR. At a typical concentration of 0.05 M there are less than 5% impurities, and all spectral data corroborate the proposed structure of polyanions.

The ^1H and ^{13}C NMR spectra of 4^{10-},$10Li^+$ at 303 K show the *t*-Bu methyl groups as three resonances with an integrated ratio of 2:1:1 (Figure 3). In the aromatic region of the $^{13}C\{^1H\}$ NMR spectrum, separate signals for the 12 quaternary carbon resonances are observed, in accordance with the DEPT experiment. Because of spectral overlap, not all carbon resonances for the aromatic CHs and quaternary sp^3 carbons of the *t*-Bu groups were resolved. In the aromatic region of the ^1H NMR spectrum, three sets of two doublets each for the three sets of six, three, and three peripheral (P) benzene rings (with *t*-Bu groups) can be identified with COSY. The three sets of the three inner benzene rings (A, B, and C) were located with COSY using three downfield singlet absorptions (A_1, B_1,and C_1), that is, the corresponding doublet/triplet absorption sets were traced to the 6.2–6.5 ppm region (Figure 3). The tentative assignment in the 6.2–6.5 ppm region (Figure 3) was further corroborated by a 2D ^1H–^1H Double Quantum (INADEQUATE) correlation: two double quantum peaks, located nearly on the $F_1 = 2F_2$ diagonal, were observed at 6.45 and 6.22 ppm. This suggests doublet/triplet spectral overlap for the protons associated with the identical benzene rings. These "diagonal" responses are accompanied by three off-diagonal correlations, which correspond to the cross peaks observed in the COSY spectrum. Consequently, 4^{10-},$10Li^+$ in THF-d_8 has 3-fold symmetry on the ^1H and ^{13}C NMR time scale at 303 K.

Charge distribution in 4^{10-} was examined using ^{13}C chemical shifts. 4^{10-} possesses 10 triarylmethyl (anionic) carbons: the unique center carbon is labeled "a" and, because of the 3-fold axis of symmetry, the remaining three sets of three carbons each are labeled "b", "c", and "d" in order of their proximity to the central "a" carbon, where "d" relates to the set of the outermost three carbons. As expected, four ^{13}C resonances are observed for these carbons (tentative assignment): 85.1 (d), 79.8 (c), 79.5 (b), 78.7 (a) ppm (Figure 3, Table I). The chemical shifts for the corresponding carbons in 3^{4-},$4Li^+$ are 82.9 and 79.3 ppm (Table I). By analogy to the behavior of simpler arylmethyl carbanions, the charge is expected to be delocalized to the benzene rings, in particular to all carbons which are located para with respect to the a–d carbons. These para carbons in the peripheral benzene rings are identified as the three most upfield quaternary carbon resonances at 132.3, 131.4, and 130.8 ppm (Figure 3). As suggested by the relative intensities, the 132.3 ppm resonance is assigned to the six peripheral benzene rings, which are attached to the d carbon; for 3^{4-},$4Li^+$, the corresponding resonance is at 133.4 ppm.[14a] For the three sets of inner benzene rings, six para resonances (two for each set) are observed in the range of 115–119 ppm (Figure 3): for 3^{4-},$4Li^+$, the corresponding resonances are at 115.8 and 113.0 ppm.[14a]

Table I. ^{13}C Chemical Shifts (ppm) for Triarylmethyl (Anionic) Carbons for Carbopolyanions in THF-d_8 at 303 K

1^-,Li^+	87.2[a]
2^{2-},$2Li^+$	83.0[a]
3^{4-},$4Li^+$	82.9, 79.3[a]
4^{10-},$10Li^+$	85.1, 79.8, 79.5, 78.7
5^{4-},$4Li^+$	89.1, 78.9

[a] Reference 14a.

It is evident from the preceding paragraph that the ^{13}C chemical shifts for the carbons bearing any significant negative charge are clustered and are similar for 4^{10-},$10Li^+$ and 3^{4-},$4Li^+$. Because of the linear relationship between ^{13}C chemical shift and charge,[18]

(14) (a) Rajca, A. *J. Am. Chem. Soc.* **1990**, *112*, 5889. (b) Rajca, A. *J. Am. Chem. Soc.* **1990**, *112*, 5890.
(15) Kothe, G.; Denkel, K.-H.; Summermann, W. *Angew. Chem., Int. Ed. Engl.* **1970**, *9*, 906. Luckhurst, G. R.; Pedulli, G. F. *J. Chem. Soc. B* **1971**, 329. Berson, J. A. In *The Chemistry of Quinoid Compounds*; Patai, S., Rappaport, Z., Eds.; Wiley: New York, 1988; Vol. II, Chapter 10.
(16) Montgomery, L. K.; Huffman, J. C.; Jurczak, E. A.; Grendze, M. P. *J. Am. Chem. Soc.* **1986**, *108*, 6004. Thiele, J.; Balhorn, H. *Chem. Ber.* **1904**, *37*, 1463.
(17) Rajca, A. *J. Org. Chem.* **1991**, *56*, 2557.
(18) Spiesecke, H.; Schneider, W. G. *Tetrahedron Lett.* **1961**, 468. O'Brien, D. H.; Hart, A. J.; Russell, C. R. *J. Am. Chem. Soc.* **1975**, *97*, 4410. Hunadi, R. *J. Am. Chem. Soc.* **1983**, *105*, 6889. Tolbert, L. M.; Ogle, M. E. *J. Am. Chem. Soc.* **1989**, *111*, 5958.
(19) Molecular propellers: Mislow, K. *Acc. Chem. Res.* **1976**, *9*, 26.
(20) Mixed dimers: Jackman, L. M.; Rakiewicz, E. F. *J. Am. Chem. Soc.* **1991**, *113*, 1202.
(21) Buncel, E.; Menon, B. C. *J. Org. Chem.* **1979**, *44*, 317.
(22) The preceding paper in this issue.
(23) Hellwinkel, D.; Stahl, H.; Gaa, H. G. *Angew. Chem., Int. Ed. Engl.* **1987**, *26*, 794.
(24) Electrochemistry of triarylmethyl anions: Bank, S.; Ehrlich, C. L.; Zubieta, J. A. *J. Org. Chem.* **1979**, *44*, 1454.
(25) For a review on the reductive cleavage of ethers, see: Maercker, A. *Angew. Chem., Int. Ed. Engl.* **1987**, *26*, 972.
(26) ESR spectrum of tris(4-*tert*-butylphenyl)methyl: Van der Hart, W. J. *Mol. Phys.* **1970**, *19*, 75.
(27) Quinodimethanes: Klasinc, L.; McGlynn, S. P. In *The Chemistry of Quinoid Compounds*; Patai, S., Rappaport, Z., Eds.; Wiley: New York, 1988; Vol. II, Chapter 5. Kato, S.; Morokuma, K.; Feller, D.; Davidson, E. R.; Borden, W. T. *J. Am. Chem. Soc.* **1983**, *105*, 1791. Rajca, A. Unpublished ab initio calculations at the HF/3-21G level of theory.
(28) Bersuker, I. B. *The Jahn-Teller Effect and Vibronic Interactions in Modern Chemistry*; Plenum: New York, 1984. Jahn, H. E.; Teller, E. *Proc. R. Soc. London, Ser. A* **1937**, *161*, 220.
(29) Radical anions of 1,3-dinitrobenzene: Ward, R. L. *J. Chem. Phys.* **1962**, *37*, 1405. Maki, A. H.; Geske, D. H. *J. Chem. Phys.* **1960**, *33*, 825. Rieger, P. H.; Fraenkel, G. K. *J. Chem. Phys.* **1963**, *39*, 609.
(30) Reference 21. Buncel, E.; Menon, B. In *Comprehensive Carbanion Chemistry, Part A*; Buncel, E., Durst, T., Eds.; Elsevier: Amsterdam, 1980; Chapter 3.
(31) Biselectrophoric radical anions: Becker, B.; Bohne, A.; Ehrenfreund, M.; Wohlfarth, W.; Sakata, Y.; Huber, W.; Mullen, K. *J. Am. Chem. Soc.* **1991**, *113*, 1121.
(32) Polarons: Chance, R. R.; Boudreaux, D. S.; Bredas, J.-L.; Silbey, R. In *Handbook of Conducting Polymers*; Skotheim, T. A., Ed.; Marcel Dekker: New York, 1986; Vol. II, Chapter 24.
(33) Powers, M. J.; Meyer, T. J. *Inorg. Chem.* **1978**, *17*, 2955. *J. Am. Chem. Soc.* **1980**, *102*, 1289.
(34) NMR temperature calibration: Raiford, D. S.; Fisk, C. L.; Becker, E. D. *Anal. Chem.* **1979**, *51*, 2050.
(35) Ferrocene: Diggle, J. W.; Parker, A. J. *J. Electrochem. Acta* **1973**, *18*, 976.

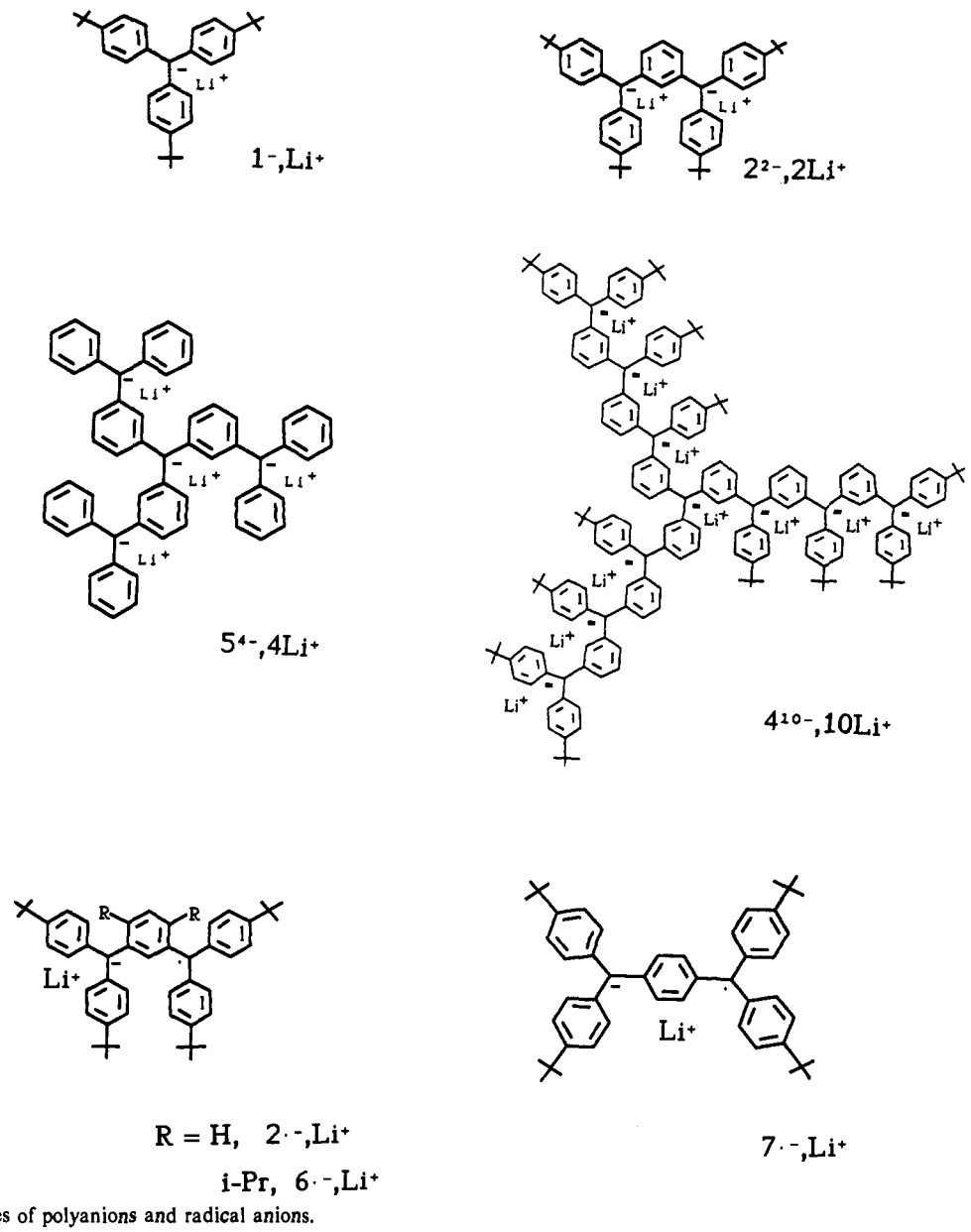

Figure 2. Structures of polyanions and radical anions.

we conclude that extending the conjugation in 1,3-connected triarylmethyl anions does not significantly perturb the electron density in the separate triarylmethyl anion units. That is, $4^{10-}.10Li^+$ is an ensemble of 10 uniformly charged triarylmethyl anion fragments.

Tetraanion $5^{4-}.4Li^+$ is used to examine the effect of removing *t*-Bu substituents on charge distribution. The ^1H NMR spectrum for $5^{4-}.4Li^+$ consists of two sets of resonances (each COSY correlated): (i) singlet, doublet, triplet, doublet, and (ii) doublet, triplet, triplet (Figure 4a).[36] The first set is assigned to the three equivalent inner benzene rings, and the second set is assigned to the six equivalent peripheral benzene rings. Using $^{13}C\{^1H\}$ and ^{13}C DEPT NMR, separate peaks for seven tertiary and five quaternary carbons are observed (Figure 4b). All tertiary ^{13}C resonances are correlated to their ^1H counterparts using HETCOR.[36] Thus, $5^{4-}.4Li^+$ in THF-d_8 has 3-fold symmetry on the ^1H and ^{13}C NMR time scale at 303 K. The ^{13}C chemical shifts for triarylmethyl (anionic) carbons are 89.1 (peripheral) and 78.9 (central) ppm (Figure 4b). The chemical shift difference between the peripheral and central carbons in tetraanions is significantly greater for $5^{4-}.4Li^+$ (10.2 ppm) compared to $3^{4-}.4Li^+$ (3.6 ppm). Therefore, *t*-Bu groups in tetraanion $3^{4-}.4Li^+$ contribute to uniform distribution of the negative charge. Both inner and peripheral benzene rings in $3^{4-}.4Li^+$ are disubstituted; in $5^{4-}.4Li^+$, the peripheral benzene rings are monosubstituted.

Low-temperature ^1H and ^{13}C NMR spectra for solutions of tetraanions $3^{4-}.4Li^+$ and $5^{4-}.4Li^+$ and decaanion $4^{10-}.10Li^+$ in THF-d_8, which also contain equivalent amounts of EtOLi, are plagued by excessive line-broadening (solvent resonances remain relatively sharp). One of the possible origins of the line-broadening is propeller isomerism for these sterically hindered triarylmethyls.[19] The major changes in the ^1H NMR spectra for $3^{4-}.4Li^+$ between 303 and 193 K are the following: (i) splitting of a single resonance for six equivalent *t*-Bu groups into two resonances each for three equivalent *t*-Bu groups, and (ii) splitting of a downfield resonance (7.23 ppm) for twelve equivalent protons in the six equivalent peripheral benzene rings into four three-proton resonances (two resonances are accidentally overlapped at 193 K). A plausible interpretation for the ^1H NMR spectrum at 193 K is that the rotation of both bis(4-*tert*-butylphenyl)methyls and peripheral benzene rings are slow on the NMR time scale at low temperatures: 3-fold symmetry is preserved on the NMR time scale. Similarly, for $5^{4-}.4Li^+$, a downfield resonance (7.2 ppm) for twelve equivalent protons (ortho) in the six equivalent peripheral benzene rings at 303 K splits into two six-proton resonances at 203 K, that

(36) ESR simulation: Janicki, S. Unpublished work from this laboratory. Kirste, B. *J. Magn. Reson.* **1987**, *73*, 213. Evans, J. C.; Morgan, P. H.; Renaud, R. H. *Anal. Chim. Acta* **1978**, *103*, 175. Monro, D. M. *Appl. Statist.* **1975**, *24*, 153.

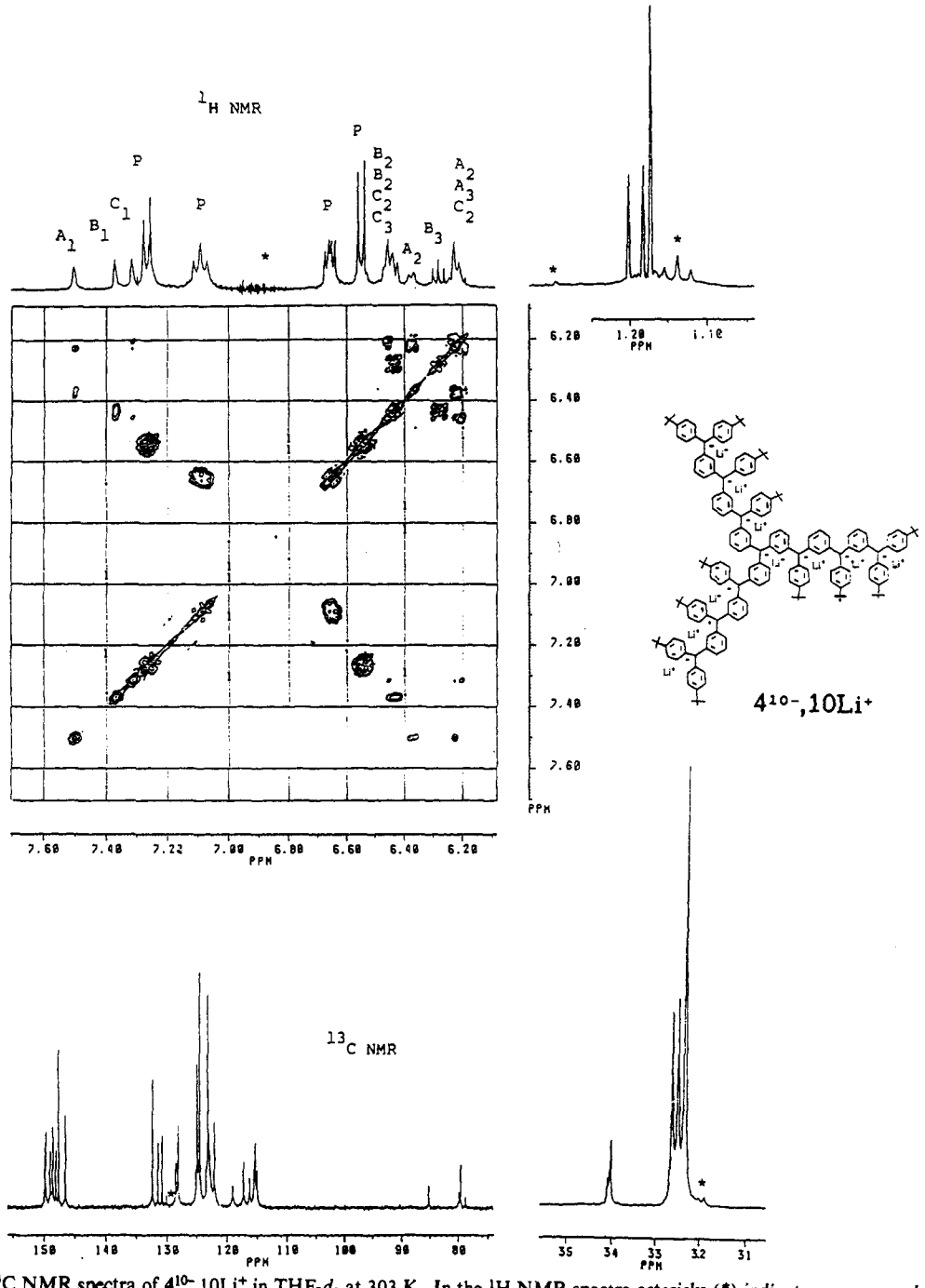

Figure 3. ^{1}H and ^{13}C NMR spectra of 4^{10-}.10Li$^+$ in THF-d_8 at 303 K. In the ^{1}H NMR spectra asterisks (*) indicate resonances due to residual protio forms of solvent, EtOLi, and instrumental artifacts. "A", "B", and "C" refer to the three sets of distinct inner meta-substituted rings. The subscripted letters refer to the corresponding multiplicity; e.g., "B_1" is assigned to a singlet in ring B. "P" indicates the resonances (all doublets) associated with the peripheral rings (bearing *t*-Bu groups). In the ^{13}C NMR spectrum not all peaks can be visually discerned in the figure; asterisks (*) indicate an unidentified impurity.

is, one of the internal rotations is slow on the NMR time scale at 203 K.

The ^{13}C chemical shifts for triarylmethyl (anionic) carbons for tetraanion 5^{4-}.4Li$^+$ and decaanion 4^{10-}.10Li$^+$ are somewhat temperature-dependent: the shift differences between the most upfield and most downfield resonances upon the change of temperature by 100 K increase by 3–5 ppm.

As expected, only one ^{6}Li and ^{7}Li resonance is observed for the Li$^+$ counterions associated with 4^{10-}.10Li$^+$ and 5^{4-}.4Li$^+$: the chemical shifts of −1.1 and −1.0 ppm, respectively, fall within the range of the chemical shifts observed for tetraanion 3^{4-}.4Li$^+$ and its smaller homologues.[14a] Integration of ^{6}Li NMR spectra at 278 K for both 3^{4-},4Li$^+$ and 4^{10-}.10Li$^+$ gives two lithiums more for the resonance associated with EtOLi compared to the resonance for lithiums associated with the polyanions. At lower temperatures, the EtOLi/polyanion integration ratios increase and the appearance of the polyanion spectra changes. For 3^{4-}.4Li$^+$, two resonances (2Li and 1Li) can be resolved at 213 K in both the ^{7}Li and ^{6}Li NMR spectra (Figure 5). A similar ^{7}Li NMR spectrum is observed for 5^{4-}.4Li$^+$ at 193 K. ^{7}Li and ^{6}Li NMR spectra for 4^{10-}.10Li$^+$ consist of two resonances at 253 K and several overlapped resonances at 213 K.

The observation of two ^{6}Li and ^{7}Li resonances for the tetraanions and several resonances for the decaanion at low temperatures might be ascribed to the equivalent lithiums in different diastereoisomers of polyanions (propeller isomerism) or nonequivalent lithiums in a single isomer of a polyanion on the NMR time scale.[19] We cannot distinguish between these two situations and other possibilities. If the solubility limitations for polyanions do not interfere, the EtOLi/polyanion lithium integrations suggest

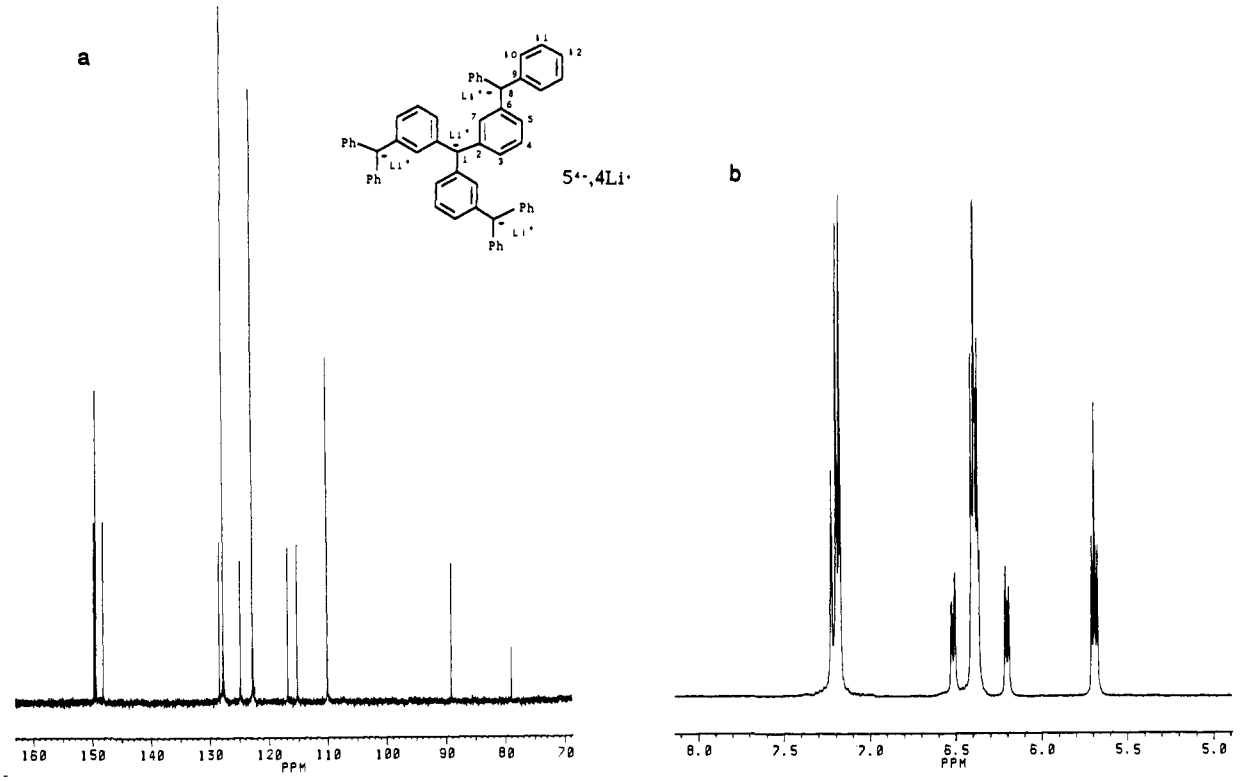

Figure 4. Partial NMR spectra for tetraanion 5^{4-},$4Li^+$ in THF-d^8 at 303 K: (a) ^{13}C NMR; (b) ^1H NMR.

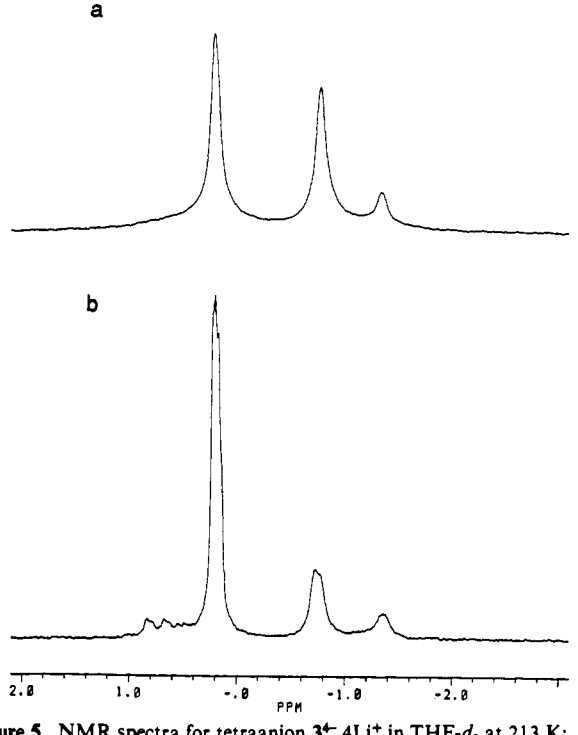

Figure 5. NMR spectra for tetraanion 3^{4-},$4Li^+$ in THF-d_8 at 213 K: (a) ^7Li NMR; (b) ^6Li NMR.

that polyanions might be effectively "free monoanions" with one of their Li^+ ions being associated with the EtOLi oligomer.[20] The important conclusion from the ^6Li and ^7Li NMR studies is that polyanions are ion multiplets at our experimental conditions.

UV–Vis. Solutions of polyanions in THF, which also contain MeLi, are examined by UV–vis spectroscopy. Notably, the spectra of polyanions are very similar and consist of a broad band with a maximum at a wavelength (λ_{max}) of about 500 nm (Figure 6, Table II). The molar absorptivities (ϵ_{max}) are approximately proportional to the number of triarylmethyl fragments (molecular charge): e.g., ϵ_{max} for a monoanion (one fragment) is 0.36×10^4 L mol^{-1} cm^{-1} and ϵ_{max} for a decaanion (ten fragments) is 3.68×10^4 L mol^{-1} cm^{-1}, which is close to $(0.36 \times 10^4$ L mol^{-1} cm$^{-1}) \times 10 = 3.6 \times 10^4$ L mol^{-1} cm^{-1}. Therefore, extending the conjugation in 1,3-connected triarylmethyl anions does not perturb the UV–vis spectra significantly. Notably, for the 1,4-connected dianion 7^{2-}.$2Li^+$, λ_{max} is 540 nm. λ_{max} and ϵ_{max} for 1^-.Li^+ and triphenylmethyllithium in THF are comparable.[21]

Table II. UV–Vis Spectral Data for Carbopolyanions in THF

	λ_{max} (nm)	$\epsilon_{max} \times 10^4$ (L mol^{-1} cm^{-1})
1^-, Li^+	504	0.36
2^{2-},$2Li^+$	481	0.78
3^{4-},$4Li^+$	485	1.43
4^{10-}.$10Li^+$	490	3.68

Table III. Cyclic Voltammetric (CV) and Differential Pulse Voltammetric (DPV) Data[a] for Monoanion 1^- and Dianion 2^{2-} (Polyanion/Polyradical Potential Range) in THF/TBAP

	CV (V ± 20 mV) E_P (ΔE_P)	DPV (V ± 20 mV) E_{DP} (ΔE_{DP})
1^-	−1.34 (0.09)	−1.37 (0.13)
2^{2-}	−1.50 (0.08)	−1.54 (0.09)
	−1.26 (0.10)	−1.33 (0.10)

[a] Potentials vs Ag wire quasi-reference electrode.

The insensitivity of λ_{max} to the extension of conjugation may be an intrinsic property of the 1,3-connected polyanions and not an artifact of ion pairing, because similar behavior is observed for 1,3-connected polyarylmethyl monoradicals and diradicals. For example, λ_{max} values for the tris(4-*tert*-butylphenyl)methyl monoradical and the related diradicals are in the 348–352 nm range.[22]

1,3-Connected polyarylmethyl in polyanions can be compared to the series of 1,4-connected polyarylmethylium ions: monocation, dication, trication, and tetracation. That is, λ_{max} changes from 432 nm for a monocation (i.e., triphenylmethylium ion) to 517 nm for a tetracation (i.e., tris[4-(diphenylmethylium)phenyl]-methylium ion).[23] Extension of conjugation for 1,4-connected polycations causes a significant red shift in UV–vis absorption.

Voltammetry. Solutions of polyanions in THF are examined by voltammetry. Tetrabutylammonium perchlorate (TBAP) is used as a supporting electrolyte.

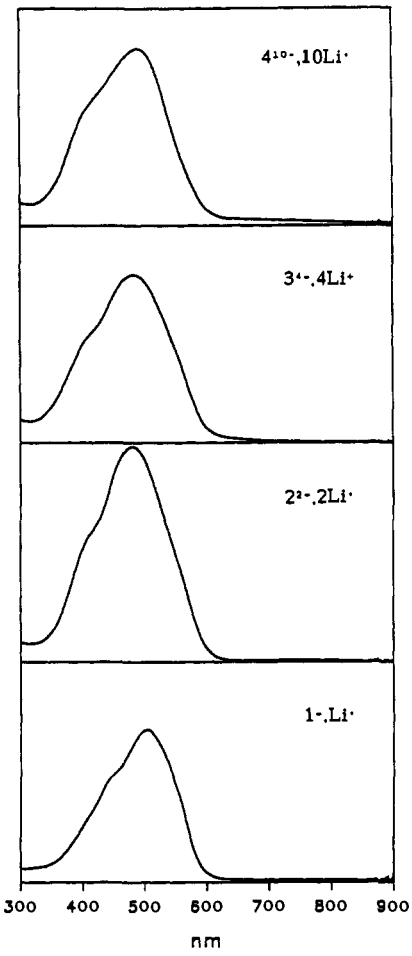

Figure 6. UV–vis spectra for polyanions 1$^-$,Li$^+$, 2^{2-},2Li$^+$, 3^{4-},4Li$^+$, and 4^{10-},10Li$^+$ in THF. The absorbance range for each spectrum is from 0 to 1.

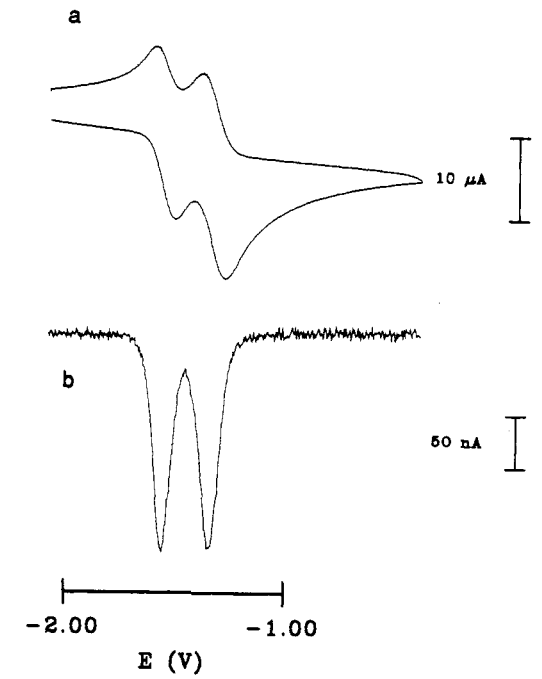

Figure 7. Cyclic voltammetry (a) and differential pulse voltammetry (b) for dianion 2^{2-} in THF/TBAP.

Cyclic voltammetric (CV) examination of monoanion 1$^-$ reveals one reversible oxidation wave at $E_p = -1.34$ V and an irreversible oxidation wave at $E_p = 0.30$ V (Table III). The waves correspond to oxidations of the anion to the radical and cation, respectively.

Scheme II

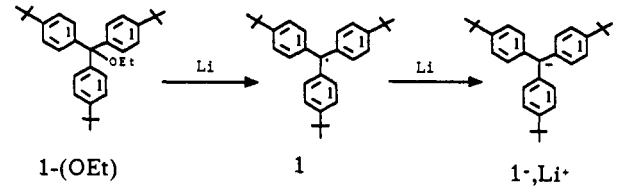

Scheme III

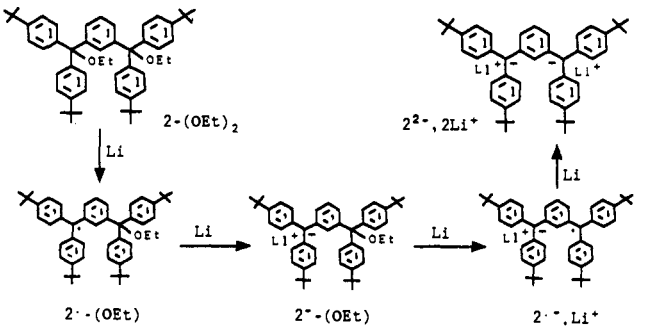

In differential pulse voltammetry (DPV), a symmetrical peak corresponding to the radical CV wave appears at $E_{DPV} = -1.37$ V. The CV data are comparable to those reported for triphenylmethyl anion.[24]

Dianion 2^{2-} possesses two reversible oxidation waves at $E_p = -1.50$ and -1.26 V in CV that correspond to the oxidation of dianion to radical anion and diradical, respectively. Similar results are obtained using DPV (Figure 7). The peak currents for the radical anion/diradical oxidation waves in CV and DPV for dianion 2^{2-} are almost identical. The oxidation waves to radical cation and dication are irreversible at our experimental conditions and are observed at about 0.3 V.[24]

When there is no interaction between the redox groups, i.e., when only the statistical factors interfere, the potential separation between the CV waves for the first and kth electron transfer should be $(2RT/F) \ln k$. For two groups, i.e., in the dianion, $k = 2$ and the potential difference should be 35.6 mV at 25 °C. The measured peak potential difference in DPV, 210 mV, in the dianion 2^{2-} is significantly larger. Therefore, there is some interaction between the triarylmethyl anion fragments. It can be estimated that a potential difference of 200 mV translates to the energy difference of about 5 kcal mol^{-1}, and it corresponds to the wavelength difference of about 50 nm in the 500-nm spectral range. In fact, the spread of λ_{max} (UV–vis) for all polyanions is only 23 nm. In a discussion of such potential (E_p) and wavelength (λ_{max}) differences, the ion-pairing effects, which cannot be quantified at the present time, would have to be considered. In summary, the NMR, UV–vis, and electrochemistry results suggest that polyanions can be viewed as ensembles of weakly interacting triarylmethyl anion units.

II. Radical Anions: Mechanism of the Cleavage of Polyethers with Lithium.[25] Stirring a 10^{-2}–10^{-3} M solution of the ether precursor 1-(OEt) in THF with lithium for 24 h yields carbanion 1$^-$.Li$^+$, and no ESR signal is detected from the resulting solution. When a 10^{-4}–10^{-5} M solution of 1-(OEt) is stirred with lithium in THF and the reaction is followed by UV–vis spectroscopy, a small amount of an intermediate with $\lambda_{max} = 350$ nm can be observed. When a 10^{-4}–10^{-5} M solution of 1-(OEt) in THF is in contact with the lithium surface without stirring, an intermediate with $\lambda_{max} = 350$ nm is formed in high yield and, subsequently, the carbanion 1$^-$.Li$^+$ with $\lambda_{max} = 504$ nm is *slowly* generated. The intermediate shows a well-resolved ESR spectrum. Both the UV–vis and ESR spectra can be assigned to tris(4-*tert*-butylphenyl)methyl radical 1$^\bullet$ (Scheme II).[26]

Further confirmation of the intermediate as tris(4-*tert*-butylphenyl)methyl radical is obtained by controlled potential electrolysis of carbanion 1$^-$ in THF/TBAP: the radical 1$^\bullet$ is formed quantitatively, and its UV–vis and ESR spectra are identical with those of the intermediate.

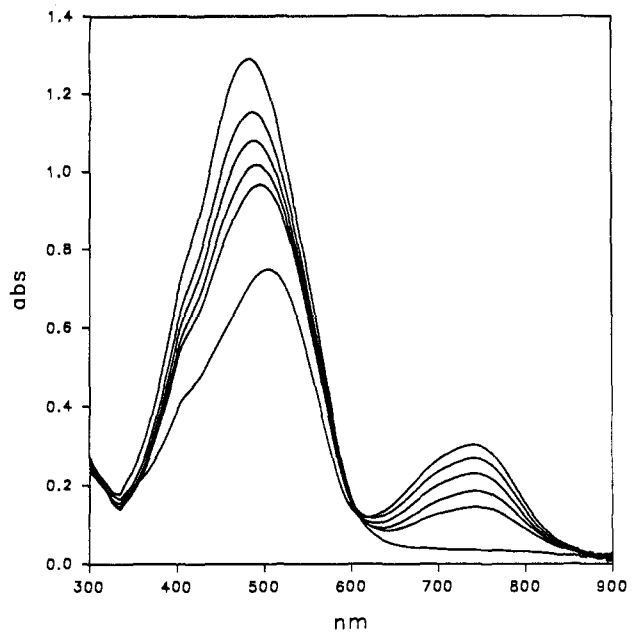

Figure 8. UV–vis spectrum following the reaction of the ether precursor **2**-$(OEt)_2$ with Li in THF.

Reaction of the ether precursor **2**-$(OEt)_2$ with lithium in THF (or THF-d_8) is followed using NMR, UV–vis, and ESR spectroscopy: typical concentrations of the ether precursor in THF are 10^{-2}, 10^{-5}, and 10^{-3} M, respectively (Scheme III).

NMR. At the intermediate stage of the reaction, a ^{1}H NMR spectrum of the reaction mixture shows resonances that may account for the mixture of the unreacted substrate **2**-$(OEt)_2$ (3 molar equiv) and the intermediate anion **2**$^-$-(OEt) (7 molar equiv): the content of the product, dianion **2**$^{2-}$.$2Li^+$, is less than the integration error (10%). Interestingly, the resonances of the anionic part of **2**$^-$-(OEt) have ^{1}H chemical shifts similar to those observed in the product dianion **2**$^{2-}$.$2Li^+$ and are quite broadened in the ^{1}H NMR spectrum and unobservable in the ^{13}C NMR spectrum (except for a broad ^{13}C resonance from the Me groups of the *t*-Bu groups). Moreover, the integration of the ^{1}H quartet of CH_3CH_2OLi at 3.73 ppm is three times the expected value compared to the amount of anion **2**$^-$-(OEt) (Scheme III). Therefore, there has to be a species present that would give rise to the additional EtOLi and, also, broaden the resonances of the "anionic" part of **2**$^-$-(OEt): e.g., paramagnetic species such as radical **2**$^•$-(OEt) or radical anion **2**$^{•-}$.Li^+ would give rise to additional EtOLi and broaden the resonances of **2**$^-$-(OEt) via electron exchange (Scheme III). Further contact of the reaction mixture with lithium metal produces relatively sharp ^{1}H and ^{13}C spectra of dianion **2**$^{2-}$.$2Li^+$ in 95+% yield.

UV–Vis. The distinction between radical **2**$^•$-(OEt) and radical anion **2**$^{•-}$.Li^+ can be made using UV–vis spectroscopy. Radical **2**$^•$-(OEt) as a triarylmethyl radical is expected to possess a λ_{max} value of approximately 350 nm.[22] Because the UV–vis spectra of monoanion **1**$^-$.Li^+ and dianion **2**$^{2-}$.$2Li^+$ are similar, the UV–vis spectra for anion **2**$^-$-(OEt), which is detected by NMR, and dianion **2**$^{2-}$.$2Li^+$ should be similar, with λ_{max} values of about 500 nm. When the reaction of the ether precursor **2**-$(OEt)_2$ with lithium in THF is followed with UV–vis spectroscopy, a transient absorption band with λ_{max} = 740 nm is observed. The absorbance of the λ_{max} = 740 nm band first increases and then decreases to zero. The absorbance of the λ_{max} = 500 nm band increases until the completion of the reaction, and λ_{max} actually changes from 495 to 481 nm upon completion of the reaction. An isosbestic point is observed (Figure 8). The λ_{max} = 740 nm band is assigned to radical anion **2**$^{•-}$,Li^+.

The λ_{max} = 740 nm assignment to the radical anion would be confirmed if the radical anion, which can be obtained by the lithium reduction of the corresponding diradical, possesses identical spectra. Because diradical **2**$^{2•}$ is unstable, diradical **6**$^{2•}$, which is stable at ambient temperature, and the ether precursor **6**-$(OMe)_2$ are used to produce the related radical anion. **6**$^{•-}$.Li^+ (Scheme IV).[22]

Scheme IV

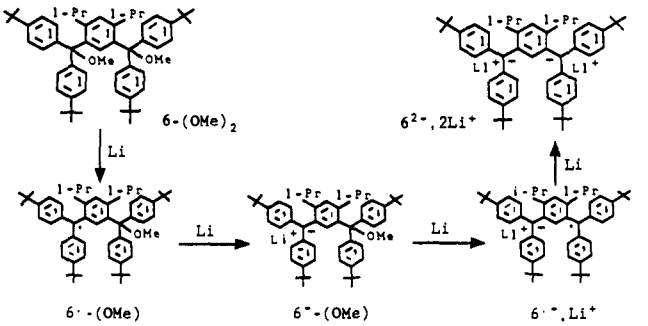

The reaction of the ether precursor **6**-$(OMe)_2$ with lithium is followed using UV–vis spectroscopy, and the observed spectral changes are analogous to those observed for the reaction of **2**-$(OEt)_2$.[37]

When the reaction of diradical **6**$^{2•}$ with lithium is followed using UV–vis, the λ_{max} = 500 nm band is formed and increases, the λ_{max} = 350 nm band of diradical **6**$^{2•}$ diminishes, and the transient λ_{max} = 770 nm band (**6**$^{•-}$.Li^+) is also observed.

ESR. The reactions of **6**-$(OMe)_2$, **6**$^{2•}$, and **2**-$(OEt)_2$ with lithium in THF are also followed using ESR. The reactions of both **6**-$(OMe)_2$ and **2**-$(OEt)_2$ give reproducible transient ESR spectra. When the reaction of diradical **6**$^{2•}$ with lithium is followed at ambient temperature in either THF or 2-MeTHF, ESR spectra are identical with those observed in the reaction of the ether precursor **6**-$(OMe)_2$ with lithium, and the peak height of the spectra first increases and then decreases as the reaction progresses.[37] When ESR spectra of the reaction in 2-MeTHF (at ambient temperature) are followed at 100 K, the peak height of the peaks associated with the triplet diradical **6**$^{2•}$ decreases, and at the same time the peak height of the resonance for the doublet species (e.g., radical anion or monoradical) first increases and then decreases as the reaction progresses.[37] Because the final product of the reduction of diradical **6**$^{2•}$ with lithium is dianion **6**$^{2-}$.$2Li^+$,[22] the only conceivable intermediate in this reaction is radical anion **6**$^{•-}$,Li^+. Since the ESR spectra obtained from the reactions of **6**-$(OMe)_2$ and **6**$^{2•}$ with lithium are identical, we conclude that the observed doublet ESR spectra correspond to **6**$^{•-}$.Li^+.

Facile observation of radical anions **6**$^{•-}$.Li^+ and **2**$^{•-}$.Li^+ is compatible with the voltammetric data: i.e., because the CV oxidation waves for the corresponding dianions are separated by about 200 mV, the disproportionation equilibria of radical anion to dianion and diradical should be in favor of radical anions.[22] We conclude that the doublet ESR spectra observed correspond to radical anions **6**$^{•-}$.Li^+ and **2**$^{•-}$.Li^+.

III. Radical Anions: Localization vs Delocalization. Simulation of the experimental ESR spectrum of **2**$^{•-}$.Li^+ indicates the following proton hyperfine couplings: a_H = 2.65 G (6 H), a_H = 1.15 G (5 H), and a_H = 2.85 G (1 H). (Hyperfine couplings from *t*-Bu groups are unresolved: line-broadening of 0.4 G is used.) Therefore, the spin density is localized in one of the triarylmethyl moieties (Figure 9).

For the reaction of the 1,4-connected ether precursor **7**-$(OEt)_2$ with lithium in THF, a transient doublet ESR spectrum is detected (Figure 10). The spectrum was assigned to radical anion **7**$^{•-}$.Li^+ using the ESR and UV–vis studies analogous to those described for 1,3-connected ether precursors and diradicals. Simulation of the ESR spectrum gives the following proton hyperfine couplings: a_H = 1.3 G (12 H) and a_H = 0.65 G (8 H). (Hyperfine couplings from *t*-Bu groups are unresolved: line-broadening of 0.3 G is used.) Therefore, the spin density in **7**$^{•-}$.Li^+ is delocalized over both triarylmethyl moieties.

The 1,3-connected π-conjugated system **2** (and its higher homologues **3** and **4**) possesses near-degenerate non-nonbonding

(37) See supplementary material.

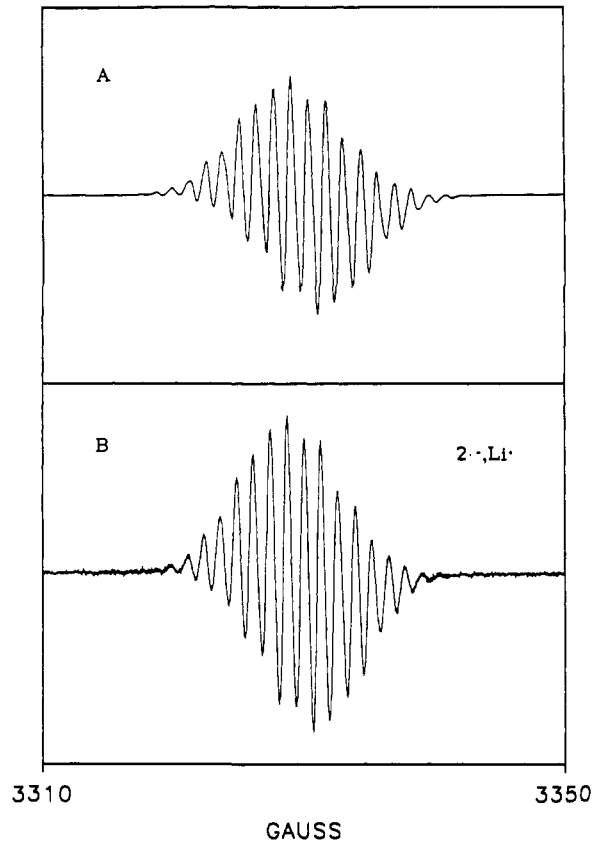

Figure 9. ESR spectrum for radical anion $2^{\bullet-}.Li^+$: (A) numerical simulation, (B) experimental; a_H = 2.65 G (6 H), a_H = 1.15 G (5 H), and a_H = 2.85 G (1 H), $g \approx 2.003$. Hyperfine couplings from *t*-Bu groups are unresolved; line-broadening of 0.4 G is used.

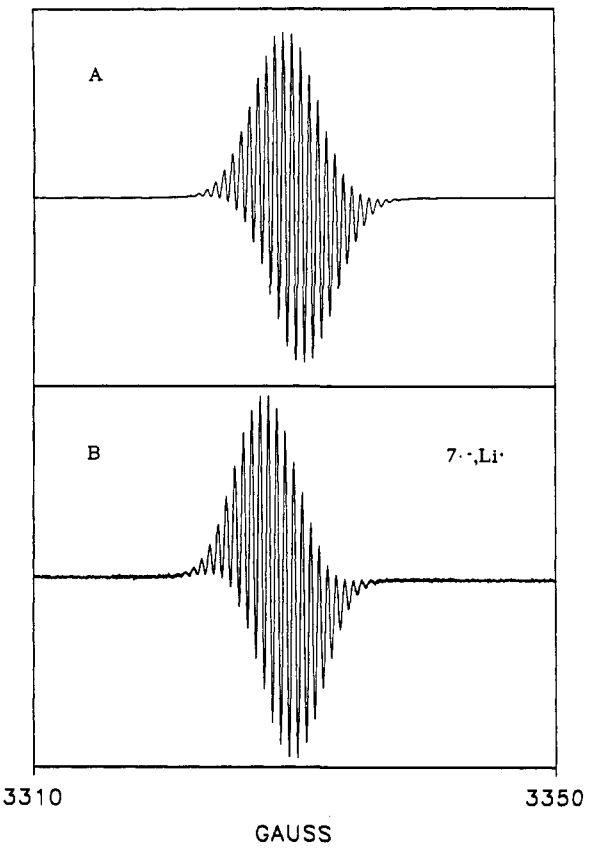

Figure 10. ESR spectrum for radical anion $7^{\bullet-}.Li^+$: (A) numerical simulation, (B) experimental; a_H = 1.3 G (12 H), a_H = 0.65 G (8 H). $g \approx 2.003$. Hyperfine couplings from *t*-Bu groups are unresolved; line-broadening of 0.3 G is used.

HOMOs. (The exact degeneracy for **2** is found using the Huckel MO model.) In the 1,4-connected system **7**, all MOs are either bonding or antibonding and, therefore, HOMO/LUMO near-degeneracies are unlikely.[27] Near-degeneracies between filled and partially filled (or empty) MOs suggest the presence of low-lying virtual excited states. Thus, large polarizability and, if the symmetries of the MOs are appropriate, second-order Jahn–Teller distortion may result.[28] Both large polarizability and JT distortion may cause localization.

Two near-degenerate nonbonding HOMOs (b_1 and a_2) are occupied by three electrons in radical anion $2^{\bullet-}$. The product of these nonbonding MOs, $b_1 \times a_2 = b_2$ (C_{2v}), suggests that a b_2 (symmetry-breaking) vibrational mode possesses a small positive (or negative) force constant; therefore, JT distortion to a lower symmetry structure may be favorable.

Large polarizability in radical anion $2^{\bullet-}$ may allow the counter ion (Li^+) or solvent to localize the negative charge. Ion pairing is known to induce localization, e.g., in 1,3-dinitrobenzene radical anions.[29] Because the corresponding triphenylmethyllithium is a solvent-separated ion pair at comparable conditions, the contribution of ion pairing to localization in $2^{\bullet-}.Li^+$ should not be significant but may not be excluded.[30]

Direct observation of localization in $2^{\bullet-}.Li^+$ and delocalization in $7^{\bullet-}.Li^+$ on the ESR time scale can be compared to analogous inorganic mixed valence compounds. Analysis of the near-IR bands in the ligand-bridged dimers $[(bpy)_2ClRu(L)RuCl(bpy)_2]^{3+}$ led Powers and Meyer to conclude that the overlap of Ru(II) and Ru(III) wave functions is less when L = pyrimidine compared to L = pyrazine; i.e., localization is preferred for 1,3-bridging.[33]

Other examples of electron localization in radical anions include polaron formation in π-conjugated polymers, biselectrophoric radical anions with alkyl spacers, and π-conjugated radical anions of diquinones.[6,31,32] In order to comment on the relationship between the topologically-induced electron localization in our molecules and these examples, we plan to carry out detailed spectroscopic studies.

Conclusions

For 1,3-connected polyarylmethyls, a relationship exists between high spin in polyradicals, localization of spin density in radical anions, and uniform charge distribution in closed-shell polyanions. The arylmethyl fragments are weakly coupled via the 1,3-bridging benzene rings but strongly coupled in the 1,4-bridging counterpart. Thus, it is possible to control electron localization/delocalization in π-conjugated systems by changing molecular topology.

The molecular models for 4^{10-} suggest that extended conformations might be preferred; thus, 4^{10-} may be a candidate for an evenly charged molecular sheet with a diameter of approximately 30 Å.

Experimental Section

Glovebox and Vacuum Lines. Air-sensitive anions were handled using either glovebox or vacuum line techniques. UV–vis and electrochemistry studies were carried out in a glovebox (Vacuum Atmospheres Co.) that was equipped with a refrigerator, solvent trap, and vacuum line. The vacuum lines were similar to the line described previously.[17]

Preparation of Polyanions. Polyanions were prepared by stirring of the ether precursor with lithium in THF. Vigorous stirring is essential for the purity of polyanions. THF was purified by distillation from Ph_2CO/Na and high-vacuum transfer from Ph_2CO/K (excess K). Lithium (Aldrich) of 98+% purity and high in sodium content was used. Lithium (95% ^{6}Li, Oak Ridge) was used for the preparation of polyanions for ^{6}Li NMR; ^{6}Li polyanions were less pure than their ^{7}Li counterparts. The tetra and higher ether precursors should be no less than 0.001 M in THF for efficient formation of polyanion. Solutions of polyanions in THF-d_8 can be stored in sealed NMR tubes in a refrigerator (−20 °C) for over a year without detectable decomposition.

NMR Spectroscopy. Samples for NMR studies were flame-sealed under vacuum in 5-mm NMR tubes. (a) Chemical shifts are reported relative to TMS (0.00 ppm) using THF-d_8 (^{1}H, 3.580 ppm and ^{13}C, 67.45 ppm) as an internal standard. A 1.0 M solution of LiCl in D_2O at 303 K was used as a 0.0 ppm reference for ^{6}Li and ^{7}Li NMR spectra; ^{6}Li and ^{7}Li chemical shifts are reproducible to within 0.2 ppm. All spectra were obtained using a Bruker WM 400 spectrometer (400.1 MHz for ^{1}H; 100.6 MHz for ^{13}C; 155.5 MHz for ^{7}Li; 85.3 MHz for ^{6}Li). Methanol

was used as a standard for the low-temperature calibration.[34]

(b) The 2D COSY, HETCOR, and 2D ^1H-^1H INADEQUATE (optimized for $J = 7$) spectra were acquired in the magnitude mode with quadrature detection in both dimensions; sine window functions were applied to the FIDs.

(c) For 4^{10-},10Li$^+$, Lorentzian-to-Gaussian transformation and exponential multiplication were applied to the FIDs prior to the Fourier transform for the one-dimensional ^1H and ^{13}C FIDs, respectively.

^1H and ^{13}C NMR spectral data at the intermediate stage of the reaction of 2-(OEt)$_2$ with lithium: ^1H NMR (THF-d_8) *303 K*, **2**$^-$(OEt) 7.37 (d, $J = 8$ Hz, 4 H), 7.19 (d, $J = 8$ Hz, 4 H), 7.1–7.3 (bs), 6.5–6.7 (bs, 4 H), 6.3–6.5 (bs, 1–2 H), 3.10 (q, $J = 7$ Hz, 2 H), 1.28 (s, 18 H), 1.18 (s, 18 H). **2**-(OEt)$_2$ 7.51 (s, 1 H), 7.31 (dd, $J = 7.7$, 1.7 Hz, 2 H), 7.25 (m, 17 H), 2.98 (q, $J = 7$ Hz, 4 H), 1.30 (s, 36 H) [EtOLi, CH_2 3.73 (m, 2 H), CH_3 1.1 (m, 3 H)]. The molar ratio of **2**-(OEt)$_2$/**2**$^-$(OEt)/EtOLi is 3/7/22 from the ^1H integration: ^{13}C NMR (THF-d_8) *303 K* 150.0, 148.5, 145.2, 144.9, 142.9, 130.1, 129.4, 129.3, 127.8, 127.3, 125.1, 124.4, 87.5, 87.1, 59.9, 59.4, 59.1, 35.0, 34.9, 32.0 (br), 31.9, 31.8, 23.4, 23.3, 16.0, 15.6.

3^{4-},4Li$^+$: ^1H NMR (THF-d_8) *268 K* 7.22 (d), 7.20 (s), 6.52 (d), 6.5–6.4 (m), 6.25 (d), 1.17 (s), *253 K* 7.21 (bs), 7.20 (s), 6.50 (d), 6.41 (s), 6.25 (s), 1.17 (s), *233 K* 7.20 (bs), 7.18 (s), 6.46 (s), 6.40 (s), 6.24 (s), 1.16 (s), *213 K* 7.40 (s), 7.30 (bs), 7.18 (s), 7.10 (bs), 6.95 (s), 6.66 (s), 6.38 (s), 6.24 (s), 1.16 (s), *193 K* 7.39 (s, 6 H), 7.15 (s, 3 H), 7.02 (s, 3 H), 6.94 (s, 3 H), 6.63 (s, 3 H), 6.35 (s, 12 H), 6.24 (s, 6 H), 1.18 (s, 27 H), 1.12 (s, 27 H); ^7Li NMR *273 K* −1.2 [EtOLi, 0.2], *253 K* −1.1 [EtOLi, 0.2], *213 K* −0.9, −1.4 [EtOLi, 0.1]; ^6Li NMR *303 K* −1.1 (br) [EtOLi, −0.1], *278 K* −1.3 (3 Li) [EtOLi, −0.1 (5 Li)], *253 K* −1.3 [EtOLi, −0.1], *233 K* −1.2 (br) [EtOLi, −0.1], *213 K* −1.0 (2 Li), −1.6 (1 Li) [EtOLi, −0.1].

4^{10-}.10Li$^+$: ^1H NMR (THF-d_8) *303 K* 7.50 (s, 3 H), 7.37 (s, 3 H), 7.31 (s, 3 H), 7.26 (d, $J = 8$ Hz, 12 H), 7.1 (bt, 12 H), 6.7 (bd, 12 H), 6.54 (d, $J = 8$ Hz, 12 H), 6.45 (m, 12 H), 6.37 (bd, 3 H), 6.28 (t, $J = 8$ Hz, 3 H), 6.22 (m, 9 H), 1.20 (s, 27 H), 1.18 (s, 27 H), 1.17 (s, 54 H) [EtOLi, 3.74 (q, $J = 7$ Hz, 20 H), 1.14 (t, $J = 7$ Hz, 30 H]; $^{13}C\{^1H\}$ and ^{13}C DEPT (135 °C) NMR *303 K* 149.7 (q), 149.6 (q), 148.9 (q), 148.5 (q), 148.4 (q), 148.0 (q), 147.5 (q), 146.5 (q), 146.4 (q), 132.3 (q), 131.4 (q), 130.8 (q), 128.5, 128.1, 124.9, 124.5, 123.1, 122.0, 119.0, 117.2, 116.2, 115.4, 115.2, 115.0, 85.1 (q), 79.8 (q), 79.5 (q), 78.7 (q), 34.0 (q), 34.0 (q), 32.6, 32.5, 32.3 [EtOLi, CH_2 59.3, 59.1, CH_3 23.2]; $^{13}C\{^1H\}$ NMR *330 K* 149.5, 149.2, 148.9, 148.74, 148.69, 148.5, 147.6, 146.5, 146.4, 146.5, 146.4, 133.0, 131.6, 131.3, 128.7, 128.5, 128.4, 125.0, 124.9, 124.5, 123.3, 122.6, 122.4, 122.1, 119.1, 117.2, 115.7, 115.3, 115.1, 84.0, 81.2, 80.0, 79.7, 34.1, 34.0, 32.54, 32.46, 32.3 [EtOLi 59.1, 23.2], *243 K* 149.8, 149.3, 148.9, 148.1, 147.7, 147.4, 146.5, 146.1, 131.6, 130.4, 127.7 (br), 124.4 (br), 122.8 (br), 118.8 (br), 116.4 (br), 114.6 (br), 87.2, 78.9, 78.4, 77.7, 34.1, 34.0, 32.7, 32.5, 32.4 [EtOLi: 59.4, 59.1, 23.4, 23.3]; ^7Li NMR *303 K* −1.1 [EtOLi, 0.2], *253 K* −1.1, −1.3 [EtOLi, 0.2], *243 K* −1.2, −1.4 [EtOLi, 0.1], *213 K* −0.9 to −1.9 (br) [EtOLi, 0.1]; ^6Li NMR *303 K* −1.2 (br) [EtOLi, −0.1 (br)], *278 K* −1.4 (9 Li) [EtOLi, −0.1 (11 Li)], *253 K* −1.4 (8 Li), −1.6 (1 Li) [EtOLi, −0.1 (11 Li)]. *243 K* −1.4, −1.6 [EtOLi, −0.1], *233 K* −1.4, −1.7 [EtOLi, −0.1], *213 K* −0.9 to −1.9 (br) [EtOLi, −0.1].

5^{4-},4Li$^+$: ^1H NMR (THF-d_8) *303 K* 7.22 (bs, 3 H), 7.18 (d, $J = 8$ Hz, 12 H), 6.51 (d, $J = 8$ Hz), 6.40–6.36 (m, 15 H), 6.21 (d, $J = 8$ Hz, 3 H), 5.69 (t, $J = 8$ Hz, 6 H) [EtOLi, 3.74 (q, $J = 7$ Hz, 8 H), 1.14 (t, $J = 7$ Hz, 12 H), *278 K* 7.22 (s), 7.18 (d), 6.55 (d), 6.36 (t), 6.19 (d), 5.65 (t) [EtOLi, 3.73 (q), 1.13 (m)], *243 K* 7.21 (s), 7.18 (bs), 6.55 (d), 6.32 (m), 6.17 (t) [EtOLi, 3.71 (m), 1.12 (m)], *223 K* 7.20 (s), 7.2 (bs), 6.53 (s), 6.32 (s), 6.16 (s), 5.60 (s) [EtOLi, 3.7 (m), 1.1 (m)], *203 K* 7.51 (s), 7.20 (s), 6.81 (s), 6.50 (s), 6.31 (s), 6.25 (s), 6.58 (s) [EtOLi, 3.7 (s), 1.1 (s)]; $^{13}C\{^1H\}$ and ^{13}C DEPT (135 °C) NMR (THF-d_8) *303 K* 149.6 (q), 149.3 (q), 148.1 (q), 128.4, 127.7, 124.8, 122.8, 116.8, 115.2, 110.0, 89.1, 78.9 [EtOLi, CH_2 59.3, 59.1, CH_3 23.3]; $^{13}C\{^1H\}$ NMR *203 K* 149.2, 148.0, 147.2, 128.3, 127.4, 124.7, 123.7, 119.3, 117.0, 114.9, 109.1, 90.8, 77.7 [EtOLi, CH_2 59.4, 59.1, CH_3 23.4]; ^7Li NMR *303 K* −1.0 [EtOLi, 0.1], *278 K* −1.0 [EtOLi, 0.1], *253 K* −1.0 [EtOLi, 0.1], *233 K* −0.9 [EtOLi, 0.1], *193 K* −0.7, −1.4 [EtOLi, 0.1].

7^{2-},2Li$^+$: ^1H NMR (THF-d_8) *303 K* 7.19 (d, $J = 8$ Hz, 8 H), 6.93 (s, 4 H), 6.42 (d, $J = 8$ Hz, 8 H), 1.15 (s, 36 H) [EtOLi, CH_2 3.65–3.90 (m, 30 H), CH_3 0.98–1.12 (m, 45 H)].

UV–Vis Spectroscopy. UV–vis absorption spectra were recorded at ambient temperature in a 2-mm pathlength quartz cell using a Perkin-Elmer Lambda 6 spectrophotometer. The spectrometer sample chamber was accessible from a glovebox. Preparations of all solutions were carried out in a glovebox under argon atmosphere. The cells were equipped with vacuum PTFE stopcocks (Kontes).

Solutions of polyanions were generated by adding an excess of Li metal into a stirred solution of the ether precursor in THF ((1–2) × 10^{-2} M). After the reaction was stirred for 1–7 days, the polyanion solution was diluted with 2 × 10^{-4} M MeLi/THF to obtain a concentration that gave an appropriate absorbance.

Molar absorptivities were obtained from Lambert–Beer law plots. The plots (five or six points) were linear in the 0.5–2.0 *A* range and, typically, correlation coefficients were $r \geq 0.997$.

Followup Experiment. A solution of the ether precursor or diradical (2 × 10^{-4} M) in 7 × 10^{-4} M MeLi/THF (or THF) was prepared in a special design cell such that the solution in a reaction compartment could be poured directly into a UV–vis quartz cell. The UV–vis spectrum of the ether precursor was recorded before a small piece of Li metal was added. After the mixture was stirred for about 5–10 min, a light pink color of solution appeared, and then the solution was transferred to the UV–vis cell compartment and the UV–vis spectrum was recorded. Stirring and recording of UV–vis spectra were alternated every 5–10 min to follow the radical anion intermediate until the reactions were completed.

Electrochemistry. All electrochemical measurements were carried out in a glovebox using the PARC Model 270 Electrochemistry System. THF was used as a solvent. The concentration of an electroactive solute was 0.001–0.003 M and the concentration of the supporting electrolyte, tetrabutylammonium perchlorate (TBAP), was 0.1–0.2 M. Three-electrode homemade voltammetric cells were used: a Ag wire quasi-reference electrode, Pt foil counter electrode, and a Pt disk working electrode (BAS). The solution volume was 2 mL. Typical CV scan rate was 200 mV/s. The differential pulse voltammetric parameters were as follows: scan rate = 4 mV/s, pulse amplitude = 10 mV, pulse width = 50 ms, pulse period = 1 s. Resistance was typically 5000 ohms, and 85% compensation using positive feedback was applied. Ferrocene (0.510 V vs SCE) was used as a reference.[35] Separation between potentials at the peaks of the oxidation and reduction CV waves was about 100 mV for both ferrocene and carbanion.

ESR Spectroscopy. A Bruker 200D SRC instrument was used to obtain X-band ESR spectra. Modified programs for numerical simulations of doublet ESR spectra were used.[36] For the generation of radical anions, reaction vessels equipped with a quartz ESR tube, which was attached to the Pyrex part of the vessel via a graded seal, and a high-vacuum stopcock (Kontes) were used.

Ether Precursor 7-(OEt)$_2$. *t*-BuLi (10.6 mL of 1.7 M solution in pentane, 18.1 mmol, Aldrich) was added to a suspension of 1,4-dibromobenzene (2.133 g, 9.04 mmol, Aldrich) in ether at −78 °C. After 50 min, solid 4,4′-di-*tert*-butylbenzophenone (2.645 g, 8.98 mmol) was added. The temperature of the cooling bath was allowed to rise to ambient temperature over a period of 3 h. Subsequently, the second portion of *t*-BuLi (10.6 mL) was added at −78 °C, and after 70 min at −78 °C, the second portion of solid 4,4′-di-*tert*-butylbenzophenone (2.655 g, 9.02 mmol) was added. The reaction mixture was allowed to attain ambient temperature over a 2-h period, and then EtOCOCl (1.73 mL, 18.1 mL) was added at 0 °C. After 16 h at ambient temperature, a concentrated aqueous solution of sodium carbonate was added. After extracting with ether, washing the ether layer with water, and drying over $MgSO_4$, concentrating in vacuo afforded 6.596 g of yellow solid. Treatment with boiling EtOH (120 mL) and filtration at ambient temperature produced 5.353 g of a light yellow solid. Column chromatography (flash silica gel, 20 psi, hexane/CH_2Cl_2, 3/1, application using hot solution in $CHCl_3$ (20 mL)) gave 2.610 g of a white solid. A sample of 0.940 g was recrystallized from hexane to produce 0.853 g of the pure product (white powder): mp 282–283 °C; FABMS (3-NBA) *m/z* (relative intensity) M^+ 722 (1), $(M - C_2H_4O)^+$ 678 (24); HR FABMS *m/z* found 722.5030, 722.5027, calcd for $C_{52}H_{66}O_2$ 722.5063; ^1H NMR ($CDCl_3$) 7.325 (s, 4 H), 7.310, 7.278 (AB, $J = 8$ Hz, 16 H), 3.073 (q, $J = 7$ Hz, 4 H), 1.296 (s, 36 H), 1.196 (t, $J = 7$ Hz, 6 H).

Acknowledgment. We gratefully acknowledge partial support by the National Science Foundation (CHEM-8912762). Acknowledgement is made to the donors of the Petroleum Research Fund, administered by the American Chemical Society, for the partial support of this research. FAB mass spectra were obtained at the Midwest Center for Mass Spectroscopy, a National Science Foundation Regional Instrumentation Facility (Grant No. CHE 8620177). We thank Professor Joseph V. Paukstelis for help with the 2D NMR spectroscopy. We thank Aaron Rigby for reproducing preparations of diether **2**-(OEt)$_2$ and tetraether **3**-(OEt)$_4$.

Registry No. **1**-(OEt), 128732-62-7; **1**$^•$, 28550-92-7; **1**$^-$,Li$^+$, 128732-61-6; **2**-(OEt)$_2$, 128732-60-5; **2**$^{•-}$,Li$^+$, 136706-47-3; **2**$^-$-(OEt), 136706-46-2; **2**$^{2-}$,2Li$^+$, 128732-59-2; **3**-(OEt)$_4$, 128732-58-1; **3**$^{4-}$,4Li$^+$, 128732-

56-9; **4**-$(OEt)_{10}$, 132885-68-8; $\mathbf{4}^{10-}$,$10Li^+$, 136706-44-0; **5**-$(OEt)_4$, 132885-79-1; $\mathbf{5}^{4-}$,$4Li^+$, 136706-45-1; **6**-$(OMe)_2$, 136575-94-5; $\mathbf{6}^{2+}$, 136575-95-6; $\mathbf{6}^{\bullet-}$,Li^+, 136706-48-4; **7**-$(OEt)_2$, 136706-43-9; $\mathbf{7}^{\bullet-}$,Li^+, 136706-49-5; $\mathbf{7}^{2-}$,$2Li^+$, 136706-50-8; 1,4-dibromobenzene, 106-37-6; 4,4'-di-*tert*-butylbenzophenone, 15796-82-4.

Supplementary Material Available: Full ^1H and ^{13}C NMR spectra at 303 K and partial COSY and HETCOR spectra for $\mathbf{5}^{4-}$,$4Li^+$; variable temperature ^1H NMR spectra for $\mathbf{3}^{4-}$,$4Li^+$; ^1H and ^{13}C NMR spectra following the reaction of **2**-$(OEt)_2$ with lithium; and ESR and UV–vis spectra following the reaction of **6**-$(OMe)_2$ and $\mathbf{6}^{2\bullet}$ with lithium (25 pages). Ordering information is given on any current masthead page.

SET Photochemistry of Flavin–Cyclopropylamine Systems. Models for Proposed Monoamine Oxidase Inhibition Mechanisms

Jong-Man Kim, Michael A. Bogdan, and Patrick S. Mariano*

Contribution from the Department of Chemistry and Biochemistry, University of Maryland, College Park, Maryland 20742. *Received June 17, 1991. Revised Manuscript Received July 29, 1991*

Abstract: Single electron transfer (SET) induced photochemical reactions of 3-methyllumiflavin (3-MLF) with the cyclopropylamines. *trans*-2-phenylcyclopropylamine (**1**) and 1-phenylcyclopropylamine (**4**), have been explored with the aim of defining the nature of and mechanisms for the reaction pathways followed. The excited-state SET processes probed in this investigation were designed to model those proposed previously for inactivation of the flavine-containing enzyme, monoamine oxidase, by these same cyclopropylamines. Irradiation of 3-MLF in an N_2-purged solution containing cyclopropylamine **4** leads to generation of the C-4a,N-5-propanodihydroflavin **14** as the major primary photoproduct. This substance, which is formed by an SET-promoted radical coupling mechanism, is transformed to the C-4a-(benzoylethyl)dihydroflavin **6** under hydrolytic conditions. Several other minor, cyclopropylamine-derived products are also generated in this reaction, again via radical pathways. In contrast, irradiation of an air-saturated solution of 3-MLF and **4** produces the epoxy ketone **8** efficiently. In this reaction, 3-MLF serves as an SET photosensitizer for the oxidative ring-opening reaction that converts **4** to **8**. Finally, the C-4a,N-5-propanodihydroflavin adducts **17** and **18** are generated along with substances arising by secondary reaction of a primary product, cinnamaldehyde (**20**), when 3-MLF is irradiated in an N_2-purged solution containing the cyclopropylamine **1**. Mechanistic aspects of these bona fide SET flavin–cyclopropylamine reactions and their possible relationship to proposals made earlier about the nature of and mechanisms for monoamine oxidase inactivation by the same cyclopropylamines are discussed.

Introduction

Cyclopropylamines are known to serve as suicide substrate inhibitors of the mammalian enzyme, monoamine oxidase (MAO).[1] This enzyme, which contains a covalently linked flavin grouping, is responsible for the catabolic conversion of biogenic amines such as norepinephrin and serotonin to their corresponding aldehydes and ammonia.[2] One member of this class of inhibitors, *trans*-2-phenylcyclopropylamine, displays potent antidepressant activity[3] owing presumably to its ability to block MAO-catalyzed decomposition of physiologically relevant biogenic amines.

Several research groups have investigated the nature of cyclopropylamine inhibition of MAO. Initially, Singer,[4] Ables,[5] and Silverman[6] speculated that the mechanism for this inactivation involves the generation of a cyclopropylimine (or related cyclopropanone) intermediate, which then undergoes bonding to the enzyme either at a cysteine thiol grouping or the N-5 position of the flavin moiety. In more recent studies of this process, Silverman[7] has accumulated evidence suggesting an alternative

Scheme I

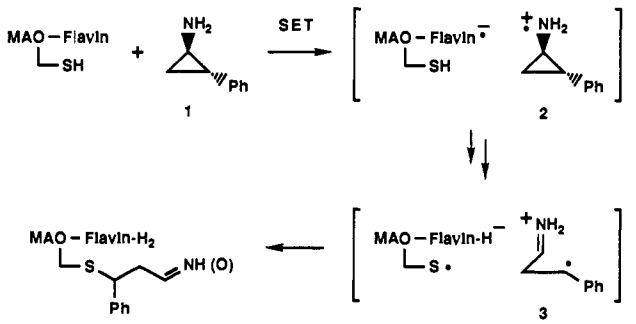

Scheme II

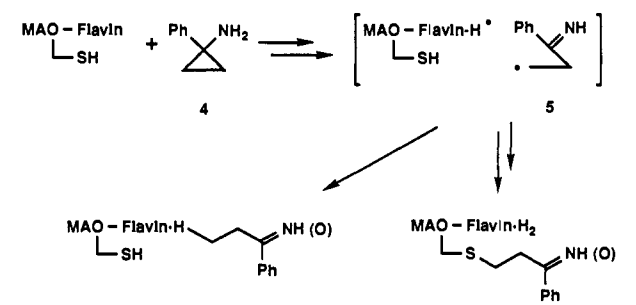

(1) (a) Erwin, V. G.; Hellerman, L. *J. Biol. Chem.* **1967**, *242*, 4230. (b) Minamiura, N.; Yasunobu, K. T. *Arch. Biochem. Biophys.* **1978**, *189*, 481. (c) Salach, J. I.; Weyler, W. *J. Biol. Chem.* **1985**, *260*, 13199. (d) Bach, A. W. J.; Lan, N. C.; Johnson, D. L.; Abell, C. W.; Bembenek, M. E.; Kwan, S.; Seeburg, P. H.; Shih, J. C. *Proc. Natl. Acad. Sci. USA* **1988**, *85*, 4934. (e) Salach, J. I.; Nagy, J. *Arch. Biochem. Biophys.* **1981**, *202*, 388.

(2) Singer, T. P. *J. Neural Transm., Suppl.* **1987**, *23*, 1.

(3) (a) Goodman, L. S.; Gilman, A. *The Pharmacological Basis of Therapeutics*, 5th ed.; MacMillan: New York, 1975; p 180. (b) Taylor, J. B.; Kennewell, P. D. *Introductory Medicinal Chemistry*; Ellis Horwood: Chichester, England, 1981; p 20.

(4) Paech, C.; Salach, J. I.; Singer, T. P. *J. Biol. Chem.* **1980**, *255*, 2700.

(5) Ables, R. H. *Enzyme-Activated Irreversible Inhibitors*; Seiler, N., Jung, M. J., Koch-Weser, J., Eds.; Elsevier: Amsterdam, 1978; pp 1–12.

(6) Silverman, R. B.; Hoffman, S. J. *Monoamine Oxidase: Structure, Functions, and Altered Functions*; Singer, T. P., VonKorff, R. W., Murphy, D. L., Eds.; Academic Press, New York, 1979; pp 71–79.

0002-7863/91/1513-9251$02.50/0